SUM-MODIFIED-LAPLACIAN FUSION METHODS EXPERIMENTED ON IMAGE STACKS OF PHOTONIC QUANTUM RING LASER DEVICES COLLECTED BY CONFOCAL SCANNING LASER MICROSCOPY

Ştefan G. STANCIU[1], Marin DRĂGULINESCU[2], George A. STANCIU[3]

In cazul anumitor tipuri de investigatii prin microscopie pot fi obtinute rezultate doar daca operatiile aferente sunt executate avand ca suport imgini cu o focalizare uniforma. Una dintre tehnicile prin care se pot obtine astfel de reprezentari este fuziunea imaginilor. In acest articol prezentam doua metode de fuziune a imaginilor bazate pe operatorul Sum-modified Laplacian (SML) care realizeaza o imagine fuzionata, compusa din mai multe imagini corespunzand sectiunilor optice achizitionate prin microscopie confocala cu baleiaj laser (CSLM). In prima metoda imaginea fuzionata este alcatuita din blocuri al caror raspuns fata de operatorul SML este maxim, iar in a doua metoda aceasta este alcatuita prin medierea ponderata a blocurilor, ponderea fiind reprezentata de raspunsul la acelasi operator.

For certain types of microscopy investigations results can be achieved only if the connected operations are performed on images of uniform focus. One of the techniques for obtaining this kind of representation is image fusion. We present two Sum-modified Laplacian (SML) image fusion methods which output a fused image built based on a stack of images collected by Confocal Scanning Laser Microscopy (CSLM). In the first method the fused image consists of blocks of highest response to SML, while in the second method it consists of mean weighted blocks, where the weight is the response to the same operator, SML.

Keywords: Image fusion, confocal scanning laser microscopy, content uniformity, sum-modified laplacian.

1. Introduction

Confocal Scanning Laser Microscopy (CSLM) provides the possibility to acquire image stacks, representing optical sections on a sample's volume [1]. An image corresponding to an optical section will in some cases contain defocused,

[1] PhD, Center for Microscopy – Microanalysis and Information Processing University Politehnica Bucharest, Romania, e-mail: sgstanciu@gmail.com
[2] Prof., Center for Microscopy – Microanalysis and Information Processing University Politehnica Bucharest, Romania
[3] Prof., Physics Department, Center for Microscopy – Microanalysis and Information Processing University Politehnica Bucharest, Romania

low contrast or over-saturated areas for the sample regions that are not in the focal plane. For certain types of investigations results can be achieved only if connected operations are performed on images of uniform focus. These types of images will allow in some cases better morphological observations of the sample details. One method for obtaining this type of representation is image fusion. By image fusion it is possible to combine relevant information from two or more images into a single composite image. The purpose of this operation is to achieve an image representing a better description of the imaged scene or object than any of the individual source images [2]. Ideally, the fusion algorithm should preserve relevant information from the fused images, suppress irrelevant parts of the image and noise and minimize any artifacts or inconsistencies in the fused image [3]. Applications of image fusion have been implemented with great success in many different fields such as remote sensing, biomedical imaging [4], and computer vision or defense systems [5]. Excellent results have also been achieved in the case of three- dimensional microscopy, where the axial resolution of the system has been enhanced by fusing images acquired at different placements of the sample [6], while in [7] wavelet based image fusion is presented as a solution which provides good results for extending the depth of field in the case of multichannel microscopy images.

Image fusion can be performed in both frequency and spatial domains. Our approach, which deals with the fusion of CSLM images, was developed on a region level basis. Lately, much attention has been focused towards region-based image fusion because of its perceived advantages : (1) Because fusion rules are based on combining regions instead of pixels, more useful tests for choosing the adequate regions from the source images, based on various properties of a region, can be implemented prior to the fusion. (2) Problems such as sensitivity to noise, blurring effects and misregistration in the case of pixel-fusion techniques, can be overcome by processing semantic regions rather than individual pixels [8].

In the case of both fusion methods that we propose, each image in the CSLM stack is divided in the same number of square regions. In the first method, which we will refer to as ‘Sum-modified Laplacian Maximum’ (SMLMAX), a focus assessment for the same region in all the images in the stack is calculated by the Sum-modified Laplacian operator (SML), and the region of the best focus is nominated to appear in the fused image. In the second method, ‘Sum-Modifed Laplacian Weighted Mean’ (SMLWM), instead of building the fused image from blocks which belong to a single image, we build it by mean averaging the blocks of all images in the stack, the contribution of each of the images to the fused image being proportional to its response to the SML operator. The motivation behind both methods is to obtain a fused image of better focus uniformity, morphological details of the structure being more visible than in any other image that contributed to the fusion.

2. Methods

2.1 Estimating focus by sum-modified-laplacian

The image fusion methods we propose are based on an image clarity measure, namely a focus measure. Once an image of the stack is divided into blocks of a certain size, for all these blocks a focus measure is calculated. Focus measures have been deeply studied in the field of autofocusing. There are two kinds of focus measures, spatial domain focus measure and frequency domain focus measure. However, frequency domain focus measures will not be used in a real-time system because of their complexity. A detailed discussion on this topic can be found in the literature [9, 10, 11, 12]. For estimating the focus of a certain region we use a spatial domain focus measure, the SML. In [13], several focus measures were compared according to the focus measure capability of distinguishing clear image blocks from blurred image blocks. The experimental results presented in [13] show that SML can provide better performance than other focus measures (Energy of Laplacian of the image, Tenenbaum's algorithm, Energy of image gradient) when the execution time is not included in the evaluation.

In [9], the authors noted that in the case of the Laplacian the second derivatives in the x- and y-directions can have opposite signs and tend to cancel each other. Therfore the focuse measure that they propose, SML, calculates the sum of the absolute values of the convolution of an image with modified Laplacian operators. The modified Laplacian takes the absolute values of the second derivatives in the Laplacian to avoid the cancellation of second derivatives in the horizontal and vertical directions that have opposite signs. The expression for the discrete approximation of ML is:

$$\nabla^2{}_{ML} f(x,y) = |2f(x,y) - f(x-step,y) - f(x+step,y)| + |2f(x,y) - f(x,y-step) - f(x,y+step)| \quad (1)$$

In order to accommodate for possible variations in the size of texture elements, the authors of [9] used a variable spacing (step) between the pixels to compute ML. We have used a step of '1'. The focus measure at a point (*x*,*y*) is computed as the sum of the modified Laplacian, in a window around the point :

$$F_{SML}^{(x,y)} = \sum_{i=x-N}^{i=x+N} \sum_{j=y-N}^{j=y+N} \nabla^2{}_{ML} f(i,j) \quad (2)$$

where the *N* parameter determines the window size used to compute the focus measure.

2.2 Fusion of Square Regions

In both of the methods we propose each of the images in the stack is divided into a set of square regions. The dimension of the square regions can be chosen

according to the type of the images that are to be fused. Higher region size is equivalent to less discriminative power between image areas, while a lower region size will bring a larger number of disturbing artifacts at the boundaries of the fused regions, also known as seams. The computational time is also directly linked to the size of the square region, larger regions being equivalent to faster processing time. Because of these aspects, a compromise should be made when choosing the size of the square region. . Usually for an image of 1024 x 1024 pixels we have obtained best results for square regions of 32 and 64 pixels.

In SMLMAX, the first method we propose, for each region, we decide its inclusion in the fused image by calculating its response to the SML operator in all the images in the stack. The block with the maximum response to the SML operator will be included in the fused image (Fig. 1), while others will be discarded.

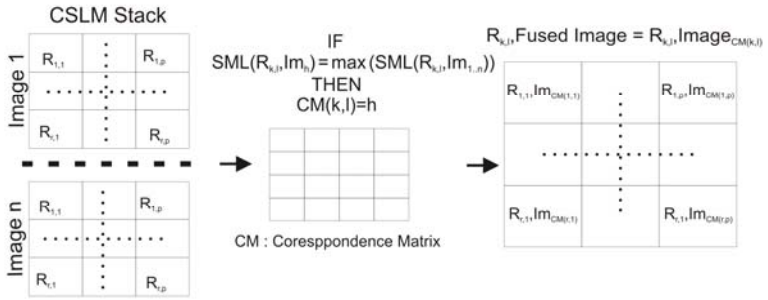

Fig. 1 SMLMAX Image fusion process

In the second method we propose, SMLWM, each of the blocks will contribute to the fused image in a certain proportion. More precisely, the contribution of the blocks, of different images in the stack, situated at the same location to the corresponding block in the fused image is proportional to their responses to the SML operator (Fig.2). Hence, the responses to the SML operator represent weights in a weighted mean based fusion image process.

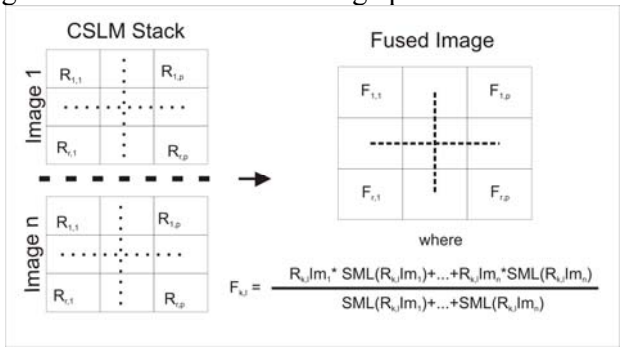

Fig. 2 SMLWM Image fusion process

3. Results

The CSLM system that was used is a Leica TCS SP CSLM. For our image fusion experiments we have investigated Photonic Quantum Ring laser devices (PQR) [14]. The PQR 'mesa' lasers are three-dimensional (3D) whispering gallery (WG) mode lasers with doughnut type Laguerre-Gaussian (LG) beam patterns. In the case of these devices it is important to obtain representations of their morphology which can be used for establishing correspondences between the photocurrents maps obtained by Laser Beam Induced Technique (LBIC), fig 3, and the physical locations where photocurrents are generated [15]. In this purpose another image fusion method was previously developed, based on a region quality metric taking into consideration the brightness, contrast and content of edges within the square regions [16], which provided good results but having also some limitations related to the pronounced seams in the resulted images.

The images of the PQR structures were obtained by scanning a 633nm (HeNe) laser beam with a maximum measured power of 10μW after the objective, at the focal plane. The objective that was used, was N PLAN L 50.0 X, with a numerical aperture of 0.5.

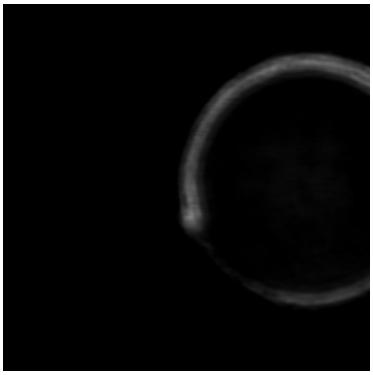

Fig. 3 Photocurrent map of a PQR device collected by LBIC.

In fig. 4 we present a stack of images obtained on the PQR devices by CSLM. The number in the top left corner depicts the numerical order of optical sections in the full series. The full series consists of 27 images. Because it is not possible to have all the regions of the device in focus at the same time due to the sample's morphology, aspects related to the geometry of the PQR devices can not be resolved from the original images obtained by CSLM. In order to resolve these issues, it is needed to have an artificial image, constructed based on the CSLM set, that would contain information from different focal planes. We have performed the image fusion algorithms described in section 2 for a number of 85 image stacks, corresponding to the same number of devices. With both methods we were able to obtain useful representations of the structures.

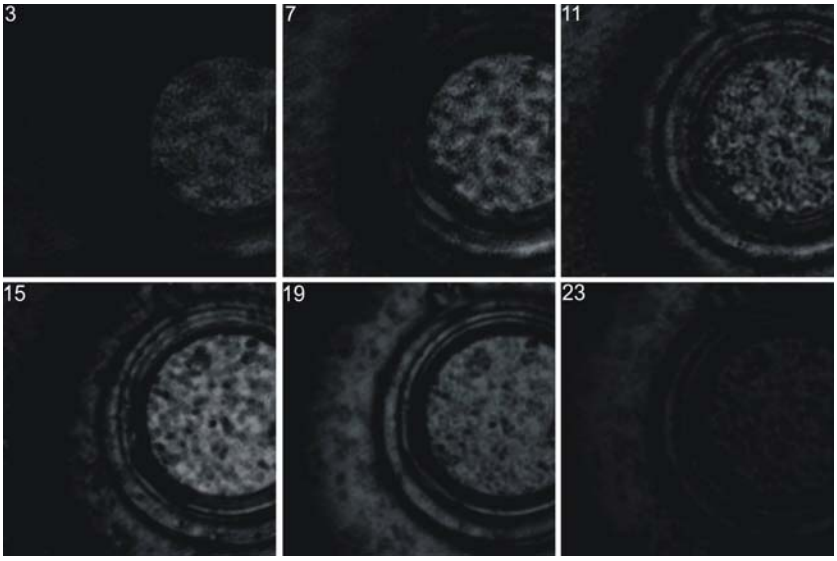

Fig. 4 Stack of images obtained by CSLM on a PQR device.

By looking at the images in the stack (fig. 4), we can observe that each one contains different details with their origin in different optical sections. If an area of the image corresponds to a region of the sample which is above the focal plane, we will most likely have a saturation effect, while if it is below the focal plane we will have an image area of low contrast. Each of the image fusion methods presented in section 2 provide an artificial image of better focus uniformity in which we have details from different focal planes, and thus more information than provided by any of the source images itself, fig. 5.

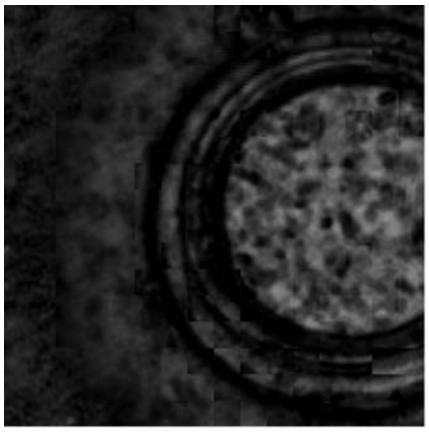

11	11	11	11	10	21	21	21	11	20	20	11	17	17	17	11
11	11	11	11	22	21	21	20	17	20	11	17	17	17	12	12
11	11	10	21	21	20	20	17	17	17	17	17	17	17	13	15
12	10	7	21	21	21	20	19	17	17	17	17	17	17	15	10
11	10	21	21	21	20	18	18	17	10	15	17	15	10	16	11
10	10	21	20	20	18	19	18	11	16	15	15	17	15	15	15
10	10	21	20	20	11	18	12	16	15	15	15	15	15	15	15
10	10	20	20	20	17	18	12	16	15	15	15	15	15	15	15
10	9	20	20	20	17	18	12	17	15	15	15	15	15	15	15
10	6	20	20	20	17	12	15	15	15	15	15	15	14	15	15
10	9	20	20	20	12	18	8	8	15	15	14	14	14	14	15
9	9	20	20	19	17	17	12	8	15	15	14	15	15	14	15
9	9	21	20	20	20	15	17	12	8	18	15	14	15	14	14
9	9	9	20	20	20	18	12	17	12	9	7	16	15	5	5
9	9	9	21	20	20	18	17	12	16	16	12	12	12	12	12
9	9	9	8	21	20	20	19	20	17	11	10	15	15	15	10

Correspondence matrix

A

B 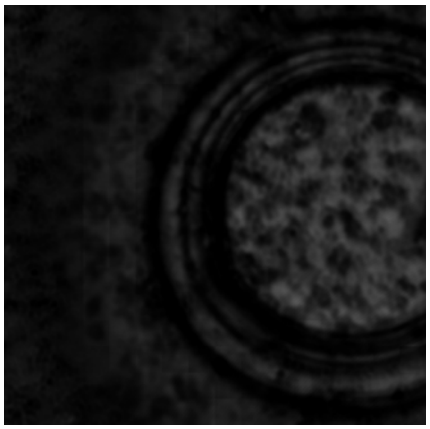

Fig. 5 a) Image obtained by SMLMAX fusion of 64*64 pixels blocks from the CSLM stack, and correspondence matrix in which each element represents the number of the image in the stack which contributes to the corresponding region in the fused image; b) Image obtained by SMLWM fusion, where weighted average has been calculated for blocks of 64*64 pixels.

The images resulted after SMLMAX image fusions have a more pronounced mosaic aspect than the images resulted after SMLWM image fusion, seams being visible at the boundaries of the fused image blocks. In the same time, these images are sharper as they preserve the high frequency details corresponding to the regions of best focus, details whose visibility is reduced in the case of the second technique because of the averaging. However, in the frame of the second technique averaging reduces not only the visibility of highy frequency details but also the contribution of noise, thus along with a blurring of the image, noise impact is also attenuated.

4. Conclusions

In this paper we describe two image fusion methods which we have used for processing CSLM image stacks collected on PQR devices. In the case of CSLM, when different regions of the investigated area are not in focus at the same time, the image will contain both focused areas, of good quality, and areas of low contrast or over saturation. By using the two presented image fusion methods we have been able obtain a representation that contains details from various focal planes. The fused image consists of image blocks of a fixed size which have been extracted or calculated from various images in the stack based on the response to the SML focus assessment operator. Both methods provide an artificial image which enables us to have a better estimate on the morphology of the studied sample in the purpose of correlating the photocurrent distribution to the device geometry than any of the source images.

Acnowledgment

The research presented in this paper has been supported by the National Program of Research, Development and Innovation PN-II-IDEI-PCE, UEFISCSU CNCSIS, Project code 1566, Contract nr. 726/2009.

R E F E R E N C E S

[1] *T. Wilson*, Confocal microscopy: Basic principles and architectures In: Diaspro A, editor. Confocal and two-photon microscopy: Foundations, applications and advances. New York: Wiley. pp. 19–38, 2001

[2] *S.G. Nikolov,* Image fusion: a survey of methods, applications, systems and interfaces, *Technical Report UoB-SYNERGY-TR02*, University of Bristol, UK, 1998

[3] *J. J. Lewis, R. J. O'Callaghan, S. G. Nikolov, D. R. Bull, N. Canagarajah,* Pixel- and region-based image fusion with complex wavelets, Information Fusion, Volume 8 , Issue 2 , Pages 119-130, 2007

[4] *Y. Kirankumar, S. Shenbaga Dev,*: Transform-based medical image fusion. International Journal of Biomedical Engineering and Technology Vol. 1, No.1 pp. 101 – 110, 2007

[5] *Z. Zhang and R. Blum*, 'Region-based image fusion scheme for concealed weapon detection', in Proceedings of the 31th Annual Conference on Information Sciences and Systems, Baltimore, USA, March 1997, pp. 168–173.

[6] *J. Swoger, P. Verveer, K. Greger, J. Huisken, and E. H. K. Stelzer,* Multi-view image fusion improves resolution in three-dimensional microscopy. Opt. Express 15, 8029-8042, 2007

[7] *B. Forster, D. Van De Ville, J. Berent, D. Sage, M. Unser*, Complex Wavelets for Extended Depth-of-Field: A New Method for the Fusion of Multichannel Microscopy Images, Microscopy Research and Technique, vol. 65, no. 1-2, pp. 33-42, 2004

[8] *S. Li and B. Yang*, Region-based multi-focus image fusion" in Image Fusion: Algorithms and Applications. Ed. Tania Stathaki, Academic Press, ISBN-10: 0123725291, ISBN-13: 978-0123725295, 2008

[9] *S.K. Nayar, Y. Nakagawa,* Shape from focus. IEEE Trans. Pattern Anal. Mach. Intell. 16 (8), 824–831, 1994

[10] *M. Subbarao, T. Choi, A. Nikzad*, Focusing Techniques. In: Proc. SPIE. Int. Soc. Opt. Eng., 163–174,1992

[11] *T. Yeo, S. Ong, S.R. Jayasooriah,* Autofocusing for tissue microscopy. Image Vision Comput. 11, 629–639, 1993

[12] *JM Geusebroek et al.,* ''Robust Autofocusing in Microscopy,'' Cytometry, 39:1–9, 2000

[13] *W. Huang, and Z. Jing,* Evaluation of focus measures in multi-focus image fusion. Pattern Recogn. Lett. 28, 4, 2007

[14] *J.C. Ahn, K. Kwak, B.H. Park, H. Y. Kang, . J.Y. Kim, O'Dae Kwon*, "Photonic Quantum Ring", *Phys. Rev. Lett*., volume 82, nr. 3, pages 536-539, 1999

[15] *G.A. Stanciu, R. Hristu, S.G. Stanciu,* O'Dae Kwon, Optical induced current technique used to investigate the photonic quantum ring laser, Proceedings of International Conference on Transparent Optical Networks, 2010.

[16] *S.G. Stanciu, D.Coltuc, R. Hristu, C. Stoichita, G.A. Stanciu*, Image fusion for photonic quantum ring laser structures investigated by confocal scanning laser microscopy, Proceedings of ICTON MW, 2009